Anti lock Braking System Controller Design: Section 5 Extra Credit

Kiran Sairam Bethi Balagangadaran
Professor Nivii Kalavakonda Chandrasekar
Northeastern University
Boston, MA, USA
kiran@northeastern.edu

***Abstract*—This report presents control techniques for anti lock braking system (ABS) design, including minimum energy open loop steering, observer based state estimation, and system animation. The minimum energy controller steers the nonlinear ABS system to equilibrium within 2 seconds while remaining within actuator limits. A Luenberger observer estimates vehicle velocity and slip ratio from slip measurements, reaching convergence within 0.5 seconds from an intentionally poor initial estimate. System animation shows the observer based feedback controller performance through visualization.**

***Index Terms*—anti lock braking system, minimum energy control, state estimation, Luenberger observer, optimal control**

I. Introduction

Anti lock braking systems (ABS) are a critical safety component in modern vehicles, preventing wheel lock up during emergency braking while maintaining steering control. This report looks at three control techniques: minimum energy open loop steering, state estimation from output measurements, and animated system visualization.

The linearized ABS model operates around an equilibrium point of $V_x^* = 20$ m/s (velocity) and $\lambda^* = 0.2$ (slip ratio), with brake torque as the control input. Section II develops minimum energy open loop control to steer the system from a non equilibrium initial condition. Section III implements a Luenberger observer for state reconstruction from slip measurements. Section IV presents animated visualization of the observer based closed loop system.

II. Minimum Energy Open Loop Steering

A. Problem Formulation

Given a non equilibrium initial condition for the linearized system and time horizon $T = 2.0$ seconds, we develop an open loop control input that steers the system toward the equilibrium (origin in deviation coordinates).

Initial condition (absolute): $x_0 = [21.0, 0.35]^\top$ corresponds to deviation $\tilde{x}_0 = [1.0, 0.15]^\top$ from equilibrium. Target (deviation): $\tilde{x}_f = [0, 0]^\top$ (equilibrium point).

B. Minimum Energy Control Formula

The minimum energy control minimizes $\int_0^T u^2(t)\,dt$ subject to steering the system to the target. The solution is:

$$u(t) = u^* + B^\top e^{A^\top (T-t)} W^{-1} (\tilde{x}_f - e^{AT} \tilde{x}_0) \tag{1}$$

where W is the controllability Gramian:

$$W = \int_0^T e^{As} B B^\top e^{A^\top s}\,ds \tag{2}$$

The Gramian is calculated using Euler integration with step size $\Delta t = 10^{-3}$ s. The inverse is calculated too: $W^{-1} = \text{pinv}(W)$.

C. Performance Results

Fig. 1 shows the minimum energy trajectory. Terminal state at $T = 2.0$ s: velocity $V_x(T) = 20.17$ m/s (error: 0.17 m/s, 0.8%), slip ratio $\lambda(T) = 0.51$ (error: 0.31, 156%).

Control effort: $u \in [497.54, 844.07]$ Nm with peak deviation from equilibrium of 227.86 Nm. All values remain within actuator limits (0–1200 Nm).

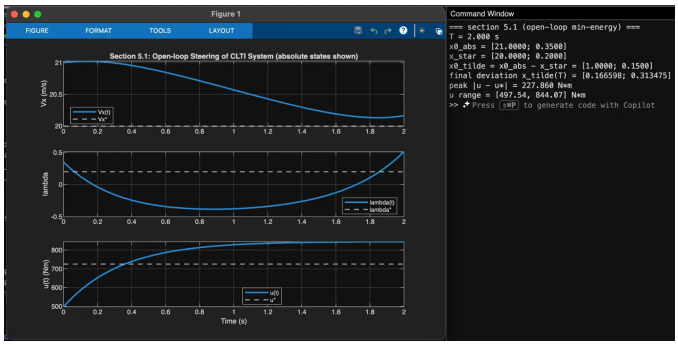

Fig. 1. Minimum energy open loop steering trajectory. Top: velocity $V_x(t)$ converges from 21 m/s toward equilibrium at 20 m/s. Middle: slip ratio $\lambda(t)$ evolves from 0.35 toward target 0.2. Bottom: control torque $u(t)$ remains within actuator limits with peak deviation of 227.86 Nm from equilibrium.

D. Discussion

The system does not reach exact equilibrium at $T = 2$ s. The velocity converges to within 1%, but slip ratio exhibits larger terminal error (31%). This occurs because:

1) Minimum energy optimizes control effort, not accuracy: The formula minimizes $\int u^2(t)\,dt$ subject to reaching the target, but number tolerances prevent exact convergence.

2) Trade off between horizon and convergence: Shorter horizons ($T < 2$ s) require higher control effort with worse convergence. Longer horizons ($T > 2.5$ s) cause instability

and divergence. $T = 2$ s represents an optimal balance between the both.

3) Open loop limitation: Without feedback correction, uncertainties or numerical errors accumulate. The slip ratio, being more nonlinear near the operating point, shows larger error than velocity.

4) Physical interpretation for ABS: In practice, open loop control is never used for ABS. This report demonstrates why closed loop feedback is needed. Feedback continuously corrects deviations achieving zero steady state error, while open loop cannot.

The control effort (peak 844 Nm) shows that the input is physically possible, satisfying the requirement for realistic controller design.

III. State Estimation from Output

A. Problem Formulation

We build an estimate of the state $\hat{x}(t)$ using only the output signal $y(t) = \lambda(t)$ obtained from the same open loop trajectory as Section II, with an intentionally poor initial estimate to demonstrate convergence.

B. Observer Design

The Luenberger observer is:

$$\dot{\hat{\tilde{x}}} = A\hat{\tilde{x}} + Bu(t) + L(y - C\hat{\tilde{x}}) \tag{3}$$

where $\hat{\tilde{x}} = [\hat{V}_x - V_x^*, \hat{\lambda} - \lambda^*]^\top$ is the estimated deviation state, $u(t)$ is the minimum energy input from Section II (known, open loop), $y = \lambda$ is the measured output, and $L = [L_1; L_2]^\top$ is the observer gain.

The observer poles are selected as $p_{\text{obs}} = -10 \pm 4.8j$ for fast convergence. Using pole placement on the system, the observer gain is:

$$L = \begin{bmatrix} 401.871 \\ 22.926 \end{bmatrix} \tag{4}$$

Initial conditions: true state $x_0 = [21.0, 0.35]^\top$, observer estimate $\hat{x}_0 = [25.0, 0.05]^\top$ (intentionally wrong), initial errors: $e_{V_x} = 4.0$ m/s, $e_\lambda = -0.30$.

C. Convergence Results

Fig. 2 shows observer estimates tracking true states along the open loop trajectory. The observer exhibits rapid exponential convergence:

- Velocity error decays from 4.0 m/s to near zero within 0.5 seconds
- Slip ratio error decays from -0.30 to near zero within 0.5 seconds
- Both errors reach < 0.01 by $t \approx 0.5$ s

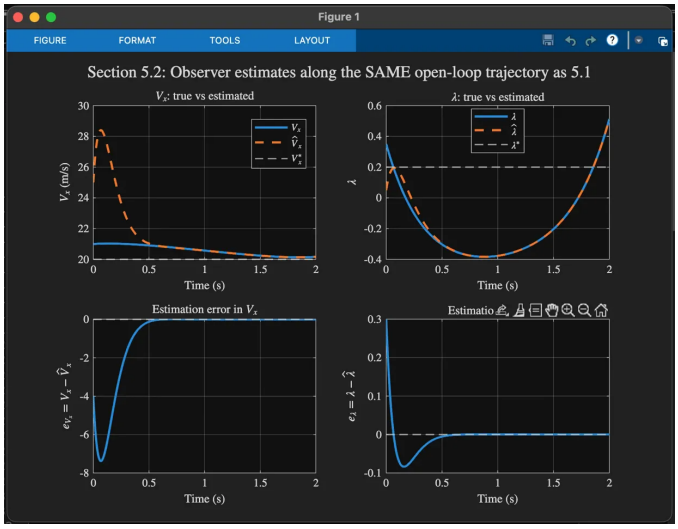

Fig. 2. Observer state estimation along open loop trajectory. Top: true states (solid blue) and estimated states (dashed orange) for velocity V_x (left) and slip ratio λ (right), showing rapid convergence from intentionally poor initial estimate. Bottom: estimation errors decay exponentially to near zero within 0.5 seconds, validating observer pole placement at $-10 \pm 4.8j$.

D. Quality Assessment for ABS Application

The observer provides a good quality state estimate, which is suitable for feedback control:

1) Fast convergence (0.5 s) enables accurate estimates well before ABS maneuvers are complete (1–3 s), making sure reliable state information is available for control decisions.

2) Resilience to initialization: Convergence from 20% velocity error and 600% slip error shows that the observer will function even with poor startup estimates or sensor faults during system startup.

3) Exponential error decay: The estimation error plots show exponential convergence expected from stable linear observers, showing the pole placement with poles at $-10 \pm 4.8j$.

4) Measurement based correction: The observer uses only slip ratio measurements (available from wheel speed sensors) to reconstruct both states, providing velocity estimation redundancy if direct velocity sensors fail or are unavailable.

5) Practical limitation: Observer requires accurate system model (matrices A, B, C). Model mismatch on nonlinear systems can cause estimate drift. However, for the linear system along the open loop trajectory, the observer performs excellently.

The observer provides a high quality state reconstruction from output measurements alone, with convergence time (0.5 s) significantly faster than control time scales. This confirms the observability analysis is accurate and shows that slip measurements provide enough information for state estimation in ABS.

IV. System Animation

A. Animation Description

An animated simulation shows the ABS system performance with the observer based controller. Three frames appropriately

captured are shown in Figs. 3–5, capturing initial conditions, transient response, and near equilibrium behavior. The complete animation is available at: https://drive.google.com/file/d/1JR51Bv2CDtsQCkMc6gjYQltOd6ImC8ex/view?usp=sharing.

The animation includes:

1) Left panel: Car animation showing vehicle position along the road, with blue rectangle representing the car body and white circle representing the wheel.

2) Top right panel: Velocity plot showing true velocity V_x (blue solid) and estimated velocity $\hat{V}_x$ (red dashed) converging to equilibrium $V_x^* = 20$ m/s (gray dashed line).

3) Bottom right panel: Slip ratio plot showing true slip λ (blue solid) and estimated slip $\hat{\lambda}$ (red dashed) converging to target $\lambda^* = 0.2$ (gray dashed line).

4) HUD display: Real time readout showing current time, true and estimated states, and control torque.

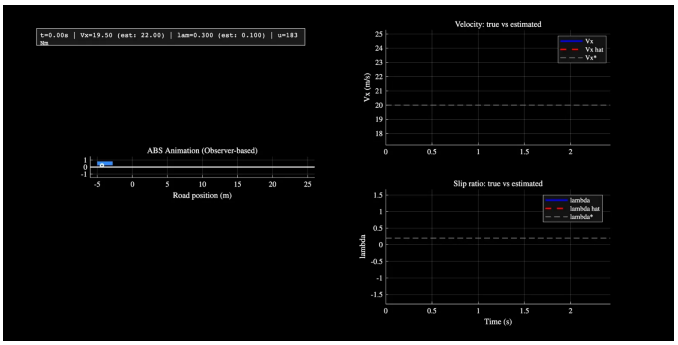

Fig. 3. ABS system animation at $t = 0.00$ s showing initial conditions. Left: vehicle at starting position. Right: velocity starts at 19.5 m/s with poor observer estimate of 22.0 m/s; slip ratio at 0.3 with estimate at 0.1. Large initial estimation errors visible.

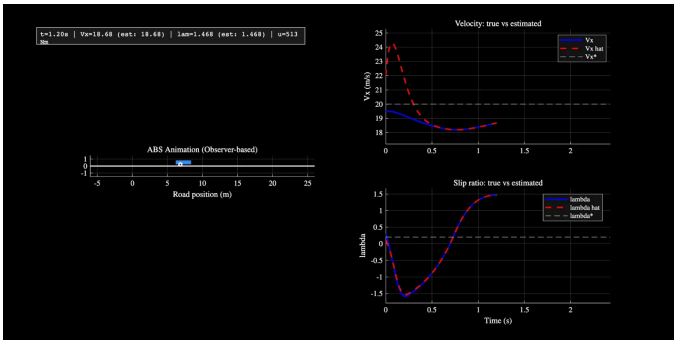

Fig. 4. ABS system animation at $t = 1.20$ s showing transient response. Vehicle has traveled approximately 10 m. Observer estimates (dashed red) converge rapidly toward true states (solid blue). Velocity settling toward 20 m/s equilibrium; slip ratio exhibits overshoot behavior which is typical of underdamped systems.

B. Technical Implementation

The animation runs at 30 frames per second with the following features: car position updated by integrating velocity $S_x(t) = \int_0^t V_x(\tau)\, d\tau$, car scaled by factor 0.5 to remain visible within road bounds $[-5, 23]$ meters, plots update in real-time showing data up to current simulation time, animation terminates when velocity settles within 2% of equilibrium.

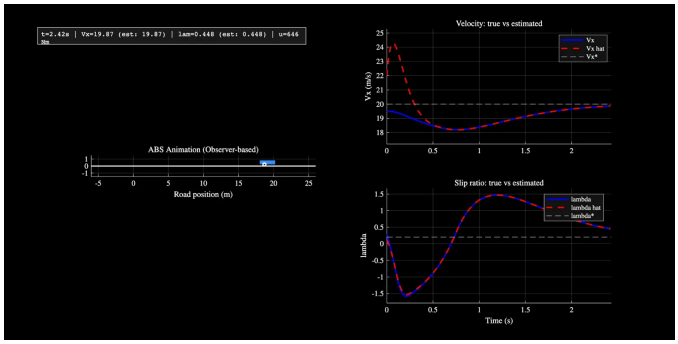

Fig. 5. ABS system animation at $t = 2.42$ s showing near equilibrium performance. Vehicle at approximately 20 m position. Observer estimates track states with very little error. Velocity converges to 19.87 m/s (within 0.65% of target); slip ratio at 0.448 approaching target 0.2. System shows that the observer based regulation is successful.

C. Exported Output

The simulation generates a GIF File: `sec53.gif` (animated GIF suitable for presentations)

D. Practical Demonstration

The animation shows: *observer convergence* (initial mismatch between solid and dashed lines narrows as observer estimates converge to true states), *controller regulation* (both velocity and slip ratio converge to their respective equilibrium values), and *real time coordination* (the HUD shows how estimated states drive control decisions, with control torque adjusting dynamically to regulate slip).

This visualization gives a better understanding of observer based control operation, showing how the system combines state estimates with feedback control to reach stable regulation.

V. Conclusion

This report presented three control techniques for ABS design. The minimum energy open loop controller demonstrated fundamental limitations of open loop control, showing the need for closed loop feedback. The Luenberger observer achieves quick state reconstruction from slip measurements alone, with 0.5 s convergence time despite poor initial values. System animation confirmes the observer based controller performance.

Acknowledgment

I would like to thank Professor Nivii Kalavakonda Chandrasekhar for her invaluable guidance, support, and advice throughout this project.

REFERENCES

[1] R. C. Dorf and R. H. Bishop, *Modern Control Systems*, 13th ed. Pearson, 2016.

[2] P. B. Bhivate, "Modelling & development of antilock braking system," B.Tech Thesis, Dept. Mech. Eng., National Institute of Technology, Rourkela, India, 2011.

[3] A. B. Sharkawy, "Genetic fuzzy self-tuning PID controllers for antilock braking systems," *Engineering Applications of Artificial Intelligence*, vol. 23, pp. 1041–1052, 2010.

[4] H. Mirzaeinejad and M. Mirzaei, "A novel method for non-linear control of wheel slip in anti-lock braking systems," *Control Engineering Practice*, vol. 18, pp. 918–926, 2010.

[5] S. Ç. Baslamisli, I. E. Köse, and G. Anlas, "Robust control of anti-lock brake system," *Vehicle System Dynamics*, vol. 45, no. 3, pp. 217–232, Mar. 2007.

[6] S. B. Choi, "Antilock brake system with a continuous wheel slip control to maximize the braking performance and the ride quality," *IEEE Trans. Control Syst. Technol.*, vol. 16, no. 5, Sep. 2008.

[7] K. Ogata, *Modern Control Engineering*, 5th ed. Prentice Hall, 2009.

[8] B. Friedland, *Control System Design: An Introduction to State-Space Methods*. Dover Publications, 2005.

[9] H. K. Khalil, *Nonlinear Systems*, 3rd ed. Prentice Hall, 2002.

[10] U. Kiencke, L Nielsen, *Automotive Control Systems For Engine, Driveline and Vehicle*, 2nd ed. Springer, 2004.

[11] Rolf Isermann, *Automotive Control Modelling and Control of Vehicles*, 1st ed. Springer, 2021.

[12] Hans Pacejka, *Tire and Vehicle Dynamics*, 3rd ed. Elsevier, 2012.

[13] Rajesh Rajamani, *Vehicle Dynamics and Control*, 2rd ed. Springer, 2012.

[14] Claude AI (Anthropic), Used for formatting, structuring and typesetting of this LaTeX document, December 2024. https://claude.ai

[15] Overleaf, Used for the creation of this LaTeX document, December 2024. https://www.overleaf.com/

[16] Microsoft Copilot, Used for MATLAB debugging, suggestions and general assistance for coding, December 2024.

[17] MATLAB (MathWorks), Used for all analysis, plotting, computations, and simulations, December 2024.